Situational Assessment for Intelligent Vehicles Based on Stochastic Model and Gaussian Distributions in Typical Traffic Scenarios

Hongbo Gao, Juping Zhu, Tong Zhang, *Member, IEEE*, Guotao Xie, Zhen Kan, *Member, IEEE*, Zhengyuan Hao, and Kang Liu

***Abstract*—In intelligent driving, situational assessment (SA) is an important technology, which helps to improve the cognitive ability of intelligent vehicles in the environment. Uncertainty analysis is very significant in situation assessment. This article proposes an SA method based on uncertainty risk analysis. Under uncertain conditions, according to the random environment model and Gaussian distribution model, the collision probability between multiple vehicles is estimated by comprehensive trajectory prediction. The proposed method considers collision probabilities of different prediction points within and outside the prediction range and obtains long-term accurate prediction results. The method is suitable for the situation risk assessment of sensor systems in the presence of unexpected dynamic obstacles, sensor failures or communication losses in traffic, and different environmental sensing accuracy. The experimental results show that in the dynamic traffic environment, the proposed scenario assessment method can not only accurately predict and assess the situation risks within the prediction range, but also provide accurate scenario risk assessment outside the prediction range.**

Manuscript received January 5, 2020; revised June 18, 2020; accepted August 15, 2020. Date of publication September 18, 2020; date of current version February 17, 2022. This work was supported in part by the Key Research and Development Plan of Anhui Province under Grant 202004a05020058; in part by the National Key Research and Development Program of China under Grant 2019YFA0706200 and Grant 2019YFB1703600; in part by the Fundamental Research Funds for the Central Universities; in part by the Science and Technology Innovation Planning Project of Ministry of Education of China; in part by NVIDIA NVAIL Program; in part by the National Natural Science Foundation of China under Grant U1804161, Grant 61751202, Grant U1813203, Grant U1801262, and Grant 61751205; in part by the Science and Technology Major Project of Guangzhou under Grant 202007030006; in part by Guangdong-Hong Kong-Macao Greater Bay Area Center for Brain Science and Brain-Inspired Intelligence Fund under Grant 2019016; in part by Key Laboratory of Advanced Perception and Intelligent Control of High-End Equipment of Ministry of Education (Anhui Polytechnic University, Wuhu, China, 241000) under Grant GDSC202007. This article was recommended by Associate Editor G. Pandey. *(Corresponding author: Tong Zhang.)*

Hongbo Gao is with the Department of Automation, University of Science and Technology of China, Hefei 230026, China, and also with the Institute of Advanced Technology, University of Science and Technology of China, Hefei 230088, China (e-mail: ghb48@ustc.edu.cn).

Juping Zhu, Zhen Kan, Zhengyuan Hao, and Kang Liu are with the Department of Automation, University of Science and Technology of China, Hefei 230026, China (e-mail: luguo_qt@163.com; zkan@ustc.edu.cn; zyhao@mail.ustc.edu.cn; xinxilk@mail.ustc.edu.cn).

Tong Zhang is with the School of Computer Science and Engineering, South China University of Technology, Guangzhou 510006, China, and also with Pazhou Lab, Guangzhou 510335, China (e-mail: tony@scut.edu.cn).

Guotao Xie is with the Department of Vehicle Engineering, Hunan University, Changsha 410082, China (e-mail: xieguotao1990@126.com).

Color versions of one or more figures in this article are available at https://doi.org/10.1109/TSMC.2020.3019512.

Digital Object Identifier 10.1109/TSMC.2020.3019512

***Index Terms*—Gaussian distributions, infinite risk assessments (IRAs), intelligent vehicles, situational assessments (SAs), uncertainty risk awareness.**

I. Introduction

IN INTELLIGENT alternative energy vehicles (IAVs), situational assessment (SA) plays a key role in understanding the environment, especially in complex traffic scenes. Through recognizing the information from the environment, the environmental meaning could be understood, and meanwhile, the future status is desired to be predicted [1]–[4]. By improving the performance of SA, the actuation systems of IAVs including brake-by-wire systems are conducive to making informed decisions. Due to the existence of the noise in various sensors, the uncertainty risks, including the loss of communication and the failure of sensors have to be faced. That is to say, system with 100% perceived reliability is hard to achieve. To perform the decision of different detection quality or IAVs safety, SA is required to consider different uncertainty risks. Moreover, the vehicle communication technology, including, vehicle to infrastructure and vehicle to vehicle in automotive technologies has become one of the important directions [5]–[8]. These technologies contribute to the provision of abundant traffic information. Importantly, the use of the information obtained could greatly promote the efficiency of the traffic. However, uncertainties caused by the noise of sensors and loss of communication should not be ignored in practice [9].

Recently, most research on IAVs focuses on lower levels to improve the performance of the vehicle safety, such as the increment of the detection accuracy as well as the enhancement of the communication reliability [10], [11]. In our study, the main goal is to guarantee the safety of IAVs by considering the uncertainty of the SA model. To deal with these issues, extensive research has been developed over the past decade [12]. Generally, support vector machines and other machine learning algorithms are widely applied in the prediction, due to the ability to solve various nonlinear problems by applying multiple features [13]–[16]. In the work of Gonzalez *et al.* [17], a model of risk assessment was proposed with the help of the inverse reinforcement learning algorithm,

to anticipate a long-term evolution of highway traffic scenarios. However, the potential risks and future uncertainties were not taken into account in the above-mentioned methods. To the best of our knowledge, these factors are crucial for the safety of IAVs [18]–[21]. As a result, the research of the uncertainty and potential risk in environmental prediction is particularly necessary. As mentioned earlier, SA using the awareness of uncertainty risk is very important to study IAVs in sustainable transportation scenarios, such as lane change [22]–[24] and intersection [25]–[27]. Nevertheless, risks with a long time and out of the prediction range are hard to be successfully assessed according to these methods.

Corresponding solutions to the deficiencies of the above methods were proposed by applying collision time (TTC) and time to lane (TTL). The dynamic characteristics of TTC and TTL are used to define risk functions, and construct the risk assessment models named the dynamic characteristics models. The model employing dynamic characteristics projects dynamic parameters of the vehicle, including relative speed, lateral acceleration of risk assessment, and distance. Lee *et al.* [28] presented a probabilistic collision risk assessment method for invisible vehicles, where the collision risk probability is evaluated based on the predicted trajectory and stochastic velocity model. Laugier *et al.* [18] pointed out that TTC is an effective method in the range of time on the straight line. In complex situations, such as intersections, the efficiency of TTC as a risk indicator will remarkably decrease. The safety field model with dynamic characteristics was considered, and meanwhile, some complex mathematical models were also proposed in [29] and [30]. First, feature relationships are defined in these models. Second, the function parameters could be adjusted by the driving data from the real world [31], [32]. In the warning system of precollision, the driving safety model has been used and proved. In the work of Kim *et al.* [33], the potential fields applying different energy functions were developed to assess risks, and appropriate decisions could be made immediately. Although the aforementioned approaches have sufficient strengths, potential risks, and future uncertainties have not been well studied.

To deal with the uncertainty of models based on dynamic characteristics, some extension schemes based on traditional methods and machine learning algorithms were adopted accordingly. In [34], the extended TTC was developed in normal traffic conditions so that the collision possibility could be evaluated by using the communication loss uncertainty. On the basis of the particle filtering, Kim *et al.* [35] proposed a new probabilistic threat assessment method employed in various complex traffic scenes without loss of generality. Unfortunately, environmental changes and collision costs were not taken into account. For better collision avoidance, Jansson and Gustafsson [36] adopted the Monte Carlo technique by transforming sensor readings with stochastic errors to the Bayesian risk. Moreover, a synthetical Bayesian method was proposed for the criticality assessment under arbitrary road environments [37]. Although the previous methods can effectively solve the uncertainty problem, the uncertainty of the sensing and position prediction is not incorporated into these studies.

With the objective to handle future potential risks of the traffic environment, many efforts were carried out to consider the uncertainty risk. Lee *et al.* [38] considered the position uncertainty of moving vehicles, and proposed a new method to predict collision so that the collision can be successfully avoided in black areas. In [39], a risk assessment scheme for collision avoidance systems was proposed based on the time sampling propagation method. This research involved estimating the uncertainty of the given vehicle's current pose along its predicted trajectory. Moreover, the target heuristic together with the maximum speed heuristic was applied to target the trajectory of unmanned aerial vehicles. In [40], by applying the classical cost function definition, Katzourakis *et al.* introduced an optimization method for autonomous driving and collision avoidance to search for the optimal track. As an alternative method, the uncertainty of sensors can be used to estimate the collision risk by employing the hidden Markov model (HMM) and Gaussian process (GP) to anticipate the collision risk. Nevertheless, the collision probability and risk beyond the scope of prediction were not mentioned. Scholliers *et al.* [4] proposed a dead reckoning system, which can predict future trajectories when the measurements of sensing are unavailable. In [41], Kalman Filter (KF) algorithm was used to process the dynamic noise covariance matrix, and thus more accurate prediction results were obtained. However, the operation of long-term prediction was not considered in this system.

The objective of this study is to assess situational risks considering uncertainties as shown in Fig. 1. In this study, the SA method is proposed based on considering uncertainty risks including environment predicting uncertainty. Based on the stochastic environment model, collision probability between multiple vehicles is estimated on the basis of trajectory prediction, behavior, and trajectory planning. The SA method considers the probabilities of collision at different predicting points, the masses, and relative speeds between the possible colliding objects. In addition, risks beyond the prediction horizon are considered with the proposition of infinite risk assessments (IRAs). This method is applied and proved to assess risks regarding unexpected obstacles in the traffic, sensor failure or communication loss, and the imperfect detection of the environment. The main contributions of this article are summarized as follows.

1) The SA method is proposed, using the risk of uncertainty by considering uncertainties in environmental prediction.
2) According to the stochastic environmental model, an equivalent form of the SA method is obtained which consists of risk assessments within the prediction horizon and risk assessments beyond the prediction horizon. Therefore, the collision probability of multiple vehicles could be estimated by comprehensive trajectory prediction.
3) Risks beyond the prediction horizon are considered with the proposition of IRAs, which is adopted to raise the forecast range.

The reminder of this article is organized as follows. Section II describes the prediction of traffic environment and collision assessment under different uncertainties. The third section introduces risk assessment. In the fourth part, the

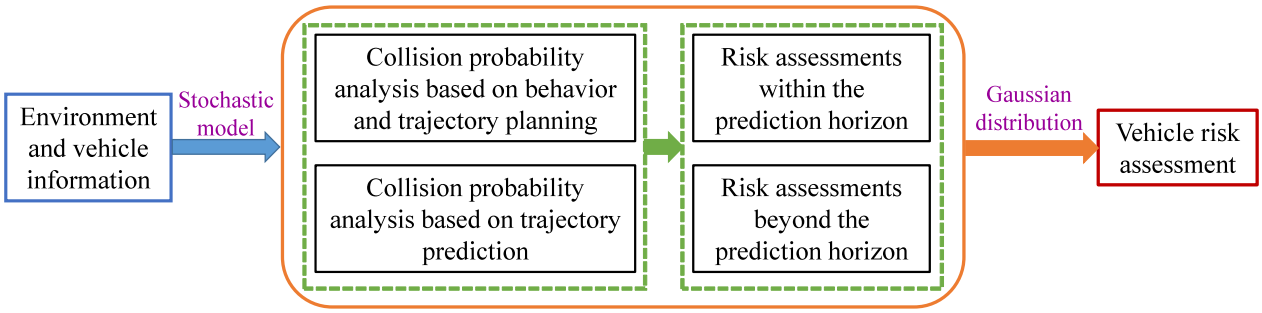

Fig. 1. Framework of the SA based on uncertainty-risk awareness.

Fig. 2. Sensor deployment of Zhihong intelligent vehicle.

uncertainty risk awareness method is applied to different scenarios. Moreover, the results are introduced and analyzed. Finally, Section V makes some concluding comments.

II. Hardware Deployment of Zhihong Intelligent Vehicle

The sensor deployment of Zhihong intelligent vehicle is shown in Fig. 2, which consists of 1 vision sensor, 7 radar sensors, and 1 integrated position/attitude sensor. The vision sensor is a camera (Mobileye C2-270), equipped on the back of the frontal mirror. The radar sensors include 1 Millimeter-wave (MMW) radar (Delphi ESR), 2 sixteen-line laser radars (Velodyne VPL-16), 2 ultrasonic radars (Softec), and 2 MMW radars (Chuhhang ARC1.01). The integrated position/attitude sensor includes global positioning system (GPS) and inertial navigation system (INS), which is from Huace. A detailed description of each sensor is shown in Table I.

The central controller is an industrial personal computer with Intel 3.3 GHz CPU, the operating system is Canonical Ltd Ubuntu 16.04, and the software development platform is Willow Garage ROS Kinetic. The central controller fulfills functions, such as sensor fusion, navigation, decision making, path planning, as well as lateral and longitudinal control.

TABLE I
Sensor Description of Zhihong Intelligent Vehicle

Sensor Type	No.	Property
Velodyne VPL-16	2	Range: 200m Horizontal Angle:360 deg Horizontal Angular Resolution: < 0.1 deg Updating: 50–200 ms (normal: 100 ms)
Softec Ultrasonic radar	2	Range:1.5 m Horizontal Angle: 70 deg Updating: 100ms
Chuhang ARC1.01	2	Range: 70m Horizontal Angle: 120 deg Angular Resolution: 1 deg Updating: 20 ms
Delphi ESR	1	Long Range: Range: 174 m Horizontal Angle: $+/-10$ deg Angular Resolution: 0.5 deg Updating: 50 ms Mid Range: Range: 60 m Horizontal Angle: $+/-45$ deg Angular Resolution: 0.1 deg Updating: 50 ms
MOBILEYE C2-270	1	Resolution Ratio: 752×480 pixels Recognition Distance: 100 m Horizontal Angular Resolution: 35 deg Updating: 50 ms
Huace CGI–610	1	Location Accuracy: 2cm (RTK) Velocity Accuracy: 0.02 m/s (Horizontal) 0.01m/s (vertical) Attitude Accuracy: 0.1 deg Frequency: 1/5/20/50/100 Hz (normal: 50 Hz)

III. Collision Assessments Under Prediction and Uncertainty

A. Stochastic Environmental Model

A traffic environment model describing the states of different objects could be applied to evaluate the traffic environment. As shown in Fig. 3, a stochastic environment model is depicted. In the stochastic model, the uncertainty is represented by a probability model, usually expressed as a probability density function (PDF). For example, the PDF could be a Gaussian distribution. In this article, a stochastic model is used to model the traffic environment.

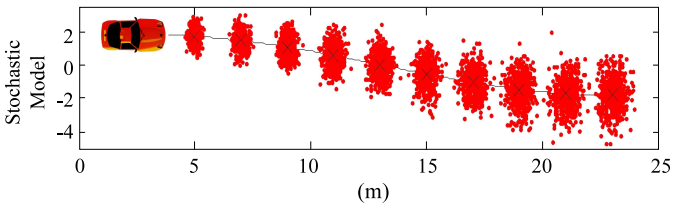

Fig. 3. Stochastic model.

In this study, $V = [x, y, v, \theta, \omega, a]$ is used to represent the vehicle states, where v stands for the vehicle velocity; $[x, y]$ stands for the vehicle position; θ stands for the yaw; ω stands for the yaw rate, and a represents the acceleration. $O(V(t))$ is used to represent the occupancy of the vehicle at time t. $s_i(V(t_0), t), t \geq t_0$ is used to represent the uncertainty states, where t_0 is the initial time, i stands for the ith object in the traffic environment. And, $i = 0$ represents that the vehicle is ego vehicle. That is, $s_0(V(t_0), t), t \geq t_0$ means the planning of the ego vehicle. Moreover, the trajectory planning is deterministic for ego vehicle. $\text{Plan}(t_0) = [s_0(V(t_0), t_0), \ldots, s_n(V(t_0), t_0)]$ stands for the initial probabilistic distribution of sensor tracking. Parameter n means the number of total objects in the traffic environment. Filtering algorithms, including extended Kalman filtering (EKF) and unscented Kalman filtering (UKF) could be used to estimate the initial sate. The future state probabilistic distribution of the vehicle can be described in the form of

$$s(V(t_0), t) = f_{\text{pre}}(V(t_0), t), \quad t_0 \leq t \leq t_0 + t_{\text{hor}} \tag{1}$$

where f_i denotes the prediction function based on the latest detecting results $V(t_0)$. t_{hor} is the prediction horizon. Notice that, the prediction function f_{pre} including method based on physics and maneuver is studied comprehensively in [42].

B. Collision Probability Using Trajectory Prediction

In the traffic scenario, the collision probability of two vehicles $(\text{Veh}_i, \text{Veh}_j)$ is $\text{Prob}(C_{\text{Veh}_i,\text{Veh}_j})$. At a specific time point, collision assessments of two vehicles using trajectory prediction could be described as follows:

$$\begin{aligned}&\text{Prob}\big(C_{\text{Veh}_i,\text{Veh}_j}(t)\big)\\ &= \int\int C\big(p_{\text{Veh}_i}(t), p_{\text{Veh}_j}(t)\big) \cdot s\big(p_{\text{Veh}_i}(t), p_{\text{Veh}_j}(t)\big)\\ &\quad dp_{\text{Veh}_i} dp_{\text{Veh}_j}, \quad t_0 \leq t \leq t_0 + t_{\text{hor}}\end{aligned} \tag{2}$$

where Veh_i and t denote the vehicle i and the time, respectively. $p_{\text{Veh}_i}(t)$ represents the predicting position of Veh_i at time t. $\text{Prob}(p_{\text{Veh}_i}(t), p_{\text{Veh}_j}(t))$ denotes the position probability of the vehicle i and j. Moreover, t_0 and t_{hor} stand for the start predicting time and the predicting interval time, respectively. Considering the shape of the vehicle, the collision index $C(p_{\text{Veh}_i}(t), p_{\text{Veh}_j}(t))$ is given by

$$\begin{aligned}&C\big(p_{\text{Veh}_i}(t), p_{\text{Veh}_j}(t)\big)\\ &= \begin{cases} 1, & O\big(p_{\text{Veh}_i}(t)\big) \cap O\big(p_{\text{Veh}_j}(t)\big) \neq 0 \\ 0, & \text{else} \end{cases}\end{aligned} \tag{3}$$

where $O(p_{\text{Veh}_i}(t))$ denotes the area covered by the vehicle i.

C. Collision Probability for Planned Maneuver and Trajectory

In our work, the collision probability of maneuvers can be evaluated within the prediction range. These actions represent abstract expressions of vehicle movements, and maneuvers are constructed as probability distributions through GP [43]. GP can represent the path as a continuous function in a probabilistic manner.

In terms of planned trajectories, $j = 0$ indicates that the trajectory of Veh_0 can be planned certainly, and collision assessment at a specific time can be written into the following equation:

$$\begin{aligned}&\text{Prob}\big(C_{\text{Veh}_i,\text{Veh}_j}(t)\big)\\ &= \int C\big(p_{\text{Veh}_i}(t), p(t)\big) \cdot s\big(p_{\text{Veh}_i}(t)\big) dp_{\text{Veh}_i}, \quad t_0 \leq t \leq t_0 + t_{\text{hor}}.\end{aligned} \tag{4}$$

IV. Risk Assessments

A. Risk Assessments Within the Prediction Horizon

According to the trajectory prediction, risks can be evaluated by considering TTC, vehicle mass, and relative speed. Therefore, the risk function for a specific predicted time is given by

$$\begin{aligned}f_{\text{risk}}\big(\text{Veh}_i(t), \text{Veh}_j(t)\big) &= \text{Prob}\big(C_{\text{Veh}_i,\text{Veh}_j}(t)\big) f_{\text{cost}}(t)\\ &\quad t_0 \leq t \leq t_0 + t_{\text{hor}}\end{aligned} \tag{5}$$

where $f_{\text{risk}}(\text{Veh}_i(t), \text{Veh}_j(t))$ is the risk at the predicting point t, and $f_{\text{cost}}(t)$ reflects the cost function with regard to the collision. The cost function $f_{\text{cost}}(t)$ is written by

$$f_{\text{cost}}(t) = \frac{1}{t_{\text{hor}}} \cdot \frac{G_i G_j}{2\big(G_i + G_j\big)} \|v_{\text{rel}}(t)\|^2 \tag{6}$$

where G_i and G_j are the weights of objects i and j, respectively; $v_{\text{rel}}(t)$ represents the relative velocity of the two vehicles; t denotes the assessment time, and $t_{\text{hor}} = t - t_0$. Moreover, $f_e = ([G_i G_j]/[2(G_i + G_j)])\|v_{\text{rel}}(t)\|^2$ is regarded as the internal energy function [44].

As a result, the risk assessment expressed by $f_{\text{risk}}(\text{Veh}_i(t_0 : t_0 + t_{\text{hor}}), \text{Veh}_j(t_0 : t_0 + t_{\text{hor}}))$ can be described as the collision prediction distribution in the future time span

$$\begin{aligned}&f_{\text{risk}}\big(\text{Veh}_i(t_0 : t_0 + t_{\text{hor}}), \text{Veh}_j(t_0 : t_0 + t_{\text{hor}})\big)\\ &= \int_{t_0}^{t_0 + t_{\max}} f_{\text{cost}} \text{Prob}\big(C_{\text{Veh}_i,\text{Veh}_j}(t)\big) dt\end{aligned} \tag{7}$$

$$\begin{aligned}&t_{\max} : \text{Prob}\big(C_{\text{Veh}_i,\text{Veh}_j}(t_{\max})\big)\\ &= \max_{t_0 \leq t \leq t_0 + t_{\text{hor}}} \text{Prob}\big(C_{\text{Veh}_i,\text{Veh}_j}(t_{\max})\big).\end{aligned} \tag{8}$$

For complex and various traffic situations, risk assessment should be taken into account in multiple vehicles. In a scene scene_i, the risk assessment of the vehicle i is written in the following form:

$$\begin{aligned}&f_{ra}^{in}(\text{Veh}_i, \text{scene}_i)\\ &= \max_j \big(f_{\text{risk}}\big(\text{Veh}_i(t_0 : t_0 + t_{\text{hor}}), \text{Veh}_j(t_0 : t_0 + t_{\text{hor}})\big)\big)\end{aligned} \tag{9}$$

with scene_i being the scene i.

Fig. 4. Without the risk assessment beyond the scope of prediction and planning horizon.

B. Risk Assessments Beyond the Prediction Horizon

Even though the risk can be assessed within the prediction range via trajectory prediction, risks beyond the time range may end immediately with collision. As can be seen from Fig. 4, a yellow vehicle approaches a white vehicle in the middle lane, while a blue vehicle (slow car) is located in the left lane. Within the scope of prediction and planning, the yellow vehicle should change to the correct lane. However, if there is no risk assessment beyond the prediction range, the yellow vehicle will be close to the road bottleneck. Consequently, the yellow vehicle must slow down. In the SA and the decision-making process, risks beyond the time limit should be considered accordingly.

The risk assessment beyond the prediction range is expressed in our work, as

$$\begin{aligned} &f_{ra}^{\infty}\left(\mathrm{Veh}_i, \mathrm{Veh}_j, \mathrm{scene}_i\right) \\ &= \int \Big[\mathrm{Prob}\left(C_{\mathrm{Veh}_i}(t)\right) \cdot \mathrm{Prob}\left(C_{\mathrm{Veh}_j}(t)\right) \\ &\qquad \times \Phi\left(\mathrm{Veh}_i, \mathrm{Veh}_j, \mathrm{scene}_i\right) \cdot f_e\Big] dp_{\mathrm{Veh}_i} dp_{\mathrm{Veh}_j} \end{aligned} \tag{10}$$

where $f_{ra}^{\infty}(\mathrm{Veh}_i, \mathrm{Veh}_j, \mathrm{scene}_i)$ denotes the risk beyond the prediction horizon, and $\Phi(\mathrm{Veh}_i, \mathrm{Veh}_j, \mathrm{scene}_i)$ is defined as below

$$\Phi\left(\mathrm{Veh}_i, \mathrm{Veh}_j, \mathrm{scene}_i\right) = \begin{cases} \frac{\Delta v_{ij}}{\Delta d_{ij}}, & \text{if } \frac{\Delta v_{ij}}{\Delta d_{ij}} > 0 \\ 0, & \text{if } \frac{\Delta v_{ij}}{\Delta d_{ij}} \leq 0 \end{cases} \tag{11}$$

where Δv_{ij} and Δd_{ij} represent the predicted relative speed and distance between the vehicle i and j, respectively.

C. Integrated Risk Assessments Using Gaussian Distributions

In our work, the SA is expressed as a comprehensive risk assessment, combining risk assessment within and outside the prediction range. In the scene scene_i, the integrated risk assessment $f_{ra}(\mathrm{Veh}_i, \mathrm{scene}_i)$ for the vehicle i is given according to

$$f_{ra}(\mathrm{Veh}_i, \mathrm{scene}_i) = f_{ra}^{in}(\mathrm{Veh}_i, \mathrm{scene}_i) + f_{ra}^{\infty}(\mathrm{Veh}_i, \mathrm{scene}_i). \tag{12}$$

Since the uncertainty of the environment is supposed to be the Gaussian distribution $\mathcal{N}$ in our work, the state of vehicles with respect to a certain time is

$$V(t) \sim \mathcal{N}\left(\mu(t), \sigma^2(t)\right) \tag{13}$$

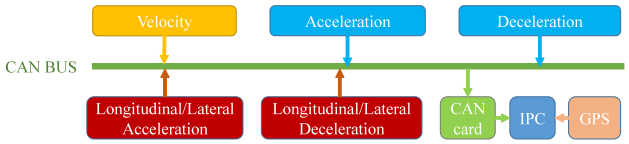

Fig. 5. Data flow of vehicle platform.

where $\mu(t)$ and $\sigma^2(t)$ are the mean and the covariance matrix of uncertainty, respectively. $V(t)$ can be obtained through sensing and tracking.

Using historical sensing and sensor tracking results, the uncertainty of the traffic environment can be predicted correspondingly. For the predicting horizon t_{hor}, the predicting results can be given by

$$\{V(t+1), V(t+2), \ldots, V(t+t_{\mathrm{hor}})\}. \tag{14}$$

Hence, a comprehensive risk assessment can be obtained by (12). The prediction of other vehicles proposed in our work is based on the combination of physical and motor methods, which can not only ensure the short-term prediction accuracy but also maintain the long-term running trend. When the onboard sensor fails or communication is lost within certain time ranges, the predicted results can be employed to update available information. The difference is that the variance of prediction information may be greater than the variance of sensors or communication devices.

The comprehensive risk assessment proposed in our work can simulate the risk of traffic obstacles. Suppose the unexpected obstacle moves in a typical mode. For example, an accidental pedestrian crossing a road should walk along a crossing modality. The following uniform Poisson process can be used to describe the probability of undesirable obstacles in traffic scenes as:

$$\mathrm{Prob}_{\mathrm{unexp}}(M_k(t_1) - M_k(t_0) \geq 1) = 1 - e^{-\varepsilon\tau} \tag{15}$$

where $(t_0, t_1]$ is the time interval and $\tau = t_1 - t_0$. $M_k(t_1) - M_k(t_0) \geq 1$ reflects that the number of undesirable obstacles is not less than one during the time interval. $\varepsilon = \gamma_k$ represents the rate parameter, which implies the number of undesirable obstacles per unite time. In addition, k denotes a scene. That is, a different parameter value ε could be selected based on each typical scene k. In terms of observations at different places or moments, the corresponding rate parameters can be obtained.

V. Experiment and Result Analysis

A. Experimental Setup

The experiments were conducted using three experimental vehicles as shown in Fig. 4, namely, yellow vehicle, blue vehicle, and white vehicle. Each vehicle was equipped with a GPS and an onboard computer to collect and record GPS position and time readings, which were used for data synchronization. Three acceleration sensors were attached to each vehicle to obtain the longitudinal and lateral acceleration, respectively, and all signals were sent to the controller area network (CAN) bus. The velocity, accelerator-pedal position, and brake-pedal ON/OFF signals were also collected from the CAN bus. During

Fig. 6. Labeling GUI. The left area displays the real time LIDAR map and images of the surrounding traffic environment. The top-right area shows the CAN data curves.

TABLE II
DETAILED INFORMATION ABOUT THE DATABASE

Labeled behavior	Number	Gender	
Right Lane-change	180	Male	61%
		Female	39%
Lane Keeping	210	Male	71%
		Female	29%
Left Lane-change	240	Male	55%
		Female	45%

the experiments, the signals from the CAN bus were transmitted to the computer through a CAN card and recorded along with GPS information in a text file. The data-collection frequency was 50 Hz. The information flow is shown in Fig. 5.

B. Experimental Process

Regarding data collection, the estimating knowledge was learned from the naturalistic driving data. The database used in this research is for driving behaviors, namely, left and right lane-change and lane keeping.

The experimental route was Changning Road, an urban four-lane road in the high-tech zone of Hefei City. The experiments were conducted under an unexpected obstacles scenario, a sensor failure scenario, a communication loss scenario, and an imperfect detection scenario. The experimental scenarios are shown in Figs. 4, 7, 10, 12, and 14, respectively.

Running information was obtained by CAN, cameras, and the LIDAR equipped on the data collecting vehicle. Running information was stored. The data collection frequency was 100 Hz. The drivers were asked to drive naturally and maintain their own driving styles.

From the collected data, the three behaviors mentioned above were labeled manually using the labeling GUI shown in Fig. 6. Part from the start to the first peak of the lane changing cases were stored in the database as lane-change episodes and used in this study.

In this experiment, the detailed information about the database is introduced in Table II. One hundred and eighty three episodes are applied as testing cases and the others as training cases.

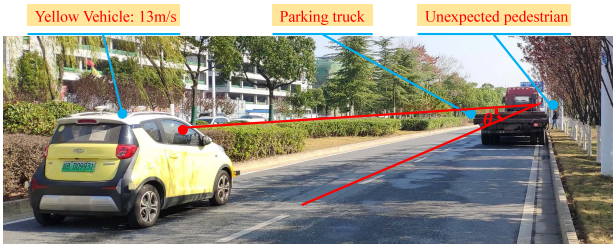

Fig. 7. Scenario regarding unexpected objects.

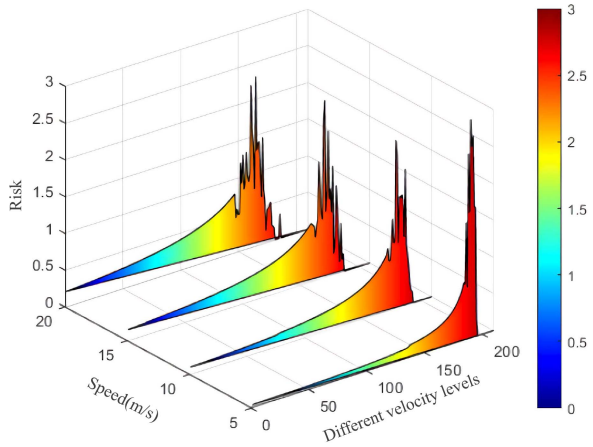

Fig. 8. Risk assessment of the unexpected pedestrians with different vehicle velocity levels.

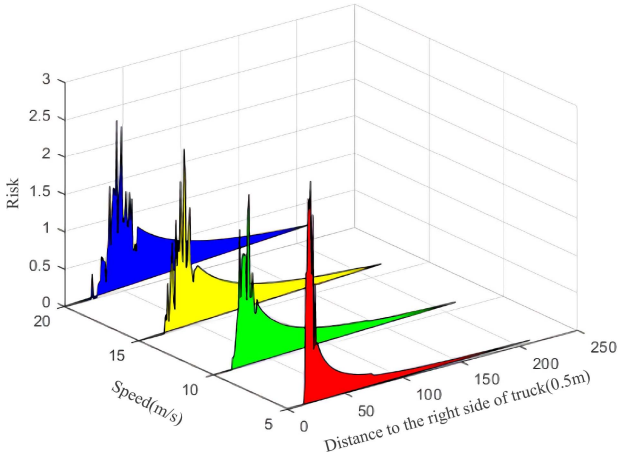

Fig. 9. Risk analysis with the distance to the right side of the truck.

C. Uncertainty Analysis in Application Scenarios

1) Situational Assessments Regarding Unexpected Objects: Especially in urban areas, undesirable objects, such as bicycles or pedestrians often occur due to incomplete perception in undetectable regions. An intuitive example is depicted in Fig. 7, in which two vehicles, a red truck and a yellow vehicle, are considered. In this case, because the red truck is parked on the right side of the road, it is hard for the yellow vehicle to discover moving obstacles ahead, for example, pedestrians crossing. It is possible that the yellow vehicle may hit pedestrians in undetectable areas. It can be worse if the yellow vehicle runs faster. In addition, as yellow vehicle advances, it becomes

more confident about whether there are pedestrians crossing the road. This kind of situation widely exists in the current urban traffic environment.

For this case, although there are no actual pedestrians crossing in front of the red truck, the yellow vehicle is required to assess the potential risk of crossing pedestrians because of the presence of undetectable areas. Because the probability of pedestrians appearing in each interval is given in (15), the collision risk for each prediction point can be expressed as

$$f_{\text{risk}}\big(\text{Veh}_i(t), \text{Veh}_j(t)\big) = \text{Prob}_{\text{unexp}} \cdot f_{ra}\big(\text{Veh}_i(t), \text{Veh}_j(t), \text{scene}_i\big) \tag{16}$$

where $f_{\text{risk}}(\text{Veh}_i(t), \text{Veh}_j(t))$ denotes the collision risk with regard to unexpected pedestrians at the predicting time t, $\text{Prob}_{\text{unexp}}$ represents the appearing probability of undesirable pedestrians, and $f_{ra}(\text{Veh}_i(t), \text{Veh}_j(t), \text{scene}_i)$ signifies the collision risk of a pedestrian crossing.

As the yellow vehicle approaches the parked red truck, the vision of the yellow vehicle keeps changing. Thus, with the continuous decrease of undetectable area, the starting intersection point of accidental pedestrians will be further enlarged in the lateral direction. Under this case, the starting intersection point is expressed in the following form:

$$w \cdot \cot\theta = L_s - L_o \tag{17}$$

where L_s and L_o denote the lateral distance between the yellow vehicle and start-crossing point, and the yellow vehicle and parking red truck, respectively. w expresses the width of the human. θ is the angle of the undetectable region.

Assume that the velocity planning of the yellow vehicle is constant and yellow vehicle is located in the middle of the lane. For the convenience of comparing results, the invariant part in SA is supposed to be a unit equal to 1. The above situation is also suitable for other scenarios in our work. The results of risk assessment are analyzed as follows. It is easy to see in Fig. 8 that, the risk regarding accidental pedestrians increases with the planned speed of the vehicle. This is in line with our daily driving experience. When we encounter a large truck parked on one side and consider the crossing of unexpected pedestrians, the risks we feel increases with the speed. To evaluate the risk of the distance on the right side of the truck, the result depicted in Fig. 9 manifests that when the yellow vehicle is far away from the right side of the truck, the corresponding risk of accidental pedestrians is increasing. Thus, the risk is maximized. After that, as the imperceptible area becomes smaller, the risk of accidental pedestrians is reduced. In addition, when the planned speed decreases, the risk decreases and the maximum risk point is gradually approaching the right side of the truck. As we know, it is also consistent with the daily experience of driving.

2) Situational Assessments Regarding Sensor Failure or Communication Loss: In this study, we assume that vehicles are all connected. The state and uncertainty information can broadcast to clouds or other vehicles [30]. When the communication is lost or the sensor fails within a certain period of time, the prediction result is used as the continuous initial state and distribution of trajectory prediction. When the communication or sensor is reestablished after a short loss, the estimation result including the uncertainty information from the detection signal is used as the latest initial state and probability distribution.

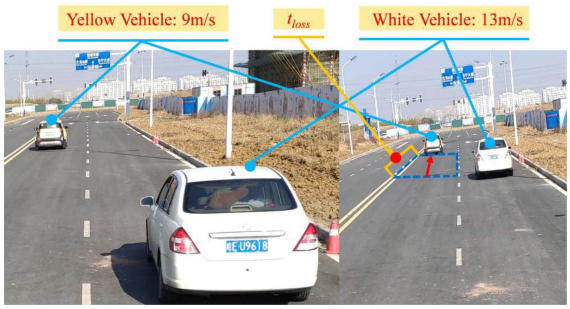

Fig. 10. Lane-keeping scenario when sensor failure or communication loss.

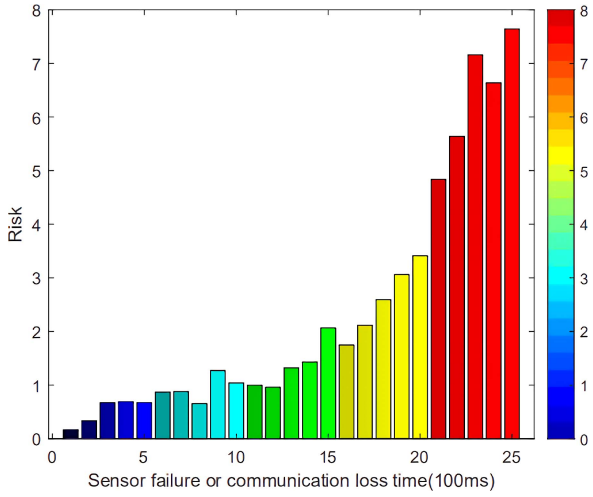

Fig. 11. Risk analysis of lane-keeping scenario when sensor failure or communication loss.

In this section, lane keeping and lane changing scenarios are studied for the application of SA in the case of sensor failure or communication loss, as shown in Figs. 9 and 10. In the above two scenarios, two vehicles are on the right of the running side. t_{loss} represents the time of sensor failure or the time of communication lost, i.e., time interval when information cannot be transported. Before t_{loss}, a dynamic Bayesian network can be employed to estimate the maneuver probability distribution as an initial maneuver distribution. The initial maneuver distribution can be expressed as follows:

$$\text{Prob}^0_{M_0} = \left(\text{Prob}^0_1, \ldots, \text{Prob}^0_n, \ldots, \text{Prob}^0_p\right) \tag{18}$$

where $\text{Prob}^0_{M_0}$ represents the maneuvers probabilistic distribution at the initial time t_0, Prob^0_n is the nth maneuver probability, and P denotes the maneuvers size.

The switching probability of maneuver in the case of sensor failure or communication loss can be defined by using the first-order Markov theory, as follows:

$$\text{Prob}^k_{M_t} = \text{Mat}\left[\text{Prob}^{k-1}_{M_t}\right]^T \tag{19}$$

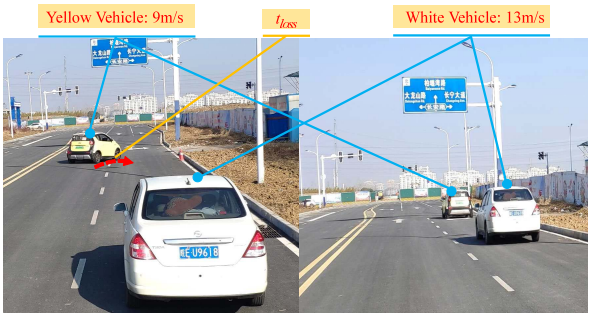

Fig. 12. Lane changing scenario when sensor failure or communication loss.

where Mat[·] stands for the probability switching matrix; $\text{Prob}_{M_t}^k$ represents the probabilistic distribution of maneuver at step k for the communication loss or sensor failure.

Therefore, under the conditions of the communication loss and sensor failure, the risk estimation could be defined as

$$f_{ra}^k(\text{Veh}_i, \text{scene}_i) = \sum_{n=1}^{P} \text{Prob}_n^k f_{ra}\left(\text{Veh}_i, \text{scene}_i | m_j = n\right) \quad (20)$$

where $f_{ra}^k(\text{Veh}_i, \text{scene}_i)$ represents the risk of the communication loss and sensor failure at step k, P represents maneuvers size of Vehicle j with $m_j = n$, and $f_{ra}^k(\text{Veh}_i, \text{scene}_i | m_j = n)$ stands for the maneuver risk of Vehicle j.

In the case of lane-keeping which is shown in Fig. 10, the yellow vehicle has no information about the red vehicle during the process of communication loss. Therefore, the yellow vehicle can only evaluate the situation using its historical data, and the prediction result is used as sensing information in an extraordinary time.

The relationship between sensor failure or communication loss time and risk is shown in Fig. 11. The result means that the risk increases with the increase of duration of communication loss or sensor failure. In the case of lane keeping, the yellow vehicle may change to other lanes when communication loss or sensor failure. That is, this risk assessment has considered uncertainty risks during communication loss or sensor failure. If the risk of uncertainty in adjacent lanes is ignored, even a white vehicle with no vehicle in the same lane can cause serious traffic accidents.

The lane change scenario is shown in Fig. 12. The information is lost when changing the lane. A prediction result could be used to replace the initial estimation information of each loss time step during the period of information loss. The prediction should use historical data.

The risk analysis of lane change scenarios in the presence of sensor failure or communication loss is shown in Fig. 13. There are two cases: one is the risks considering uncertainty prediction, and the other is the risks without considering uncertainty prediction. The results of the two cases are compared and analyzed. The comparison results imply that the risk without considering the prediction uncertainty is higher than the risk considering the prediction uncertainty, during sensor failure or lane change scenario when the prediction uncertainty is considered. Therefore, during communication loss or sensor

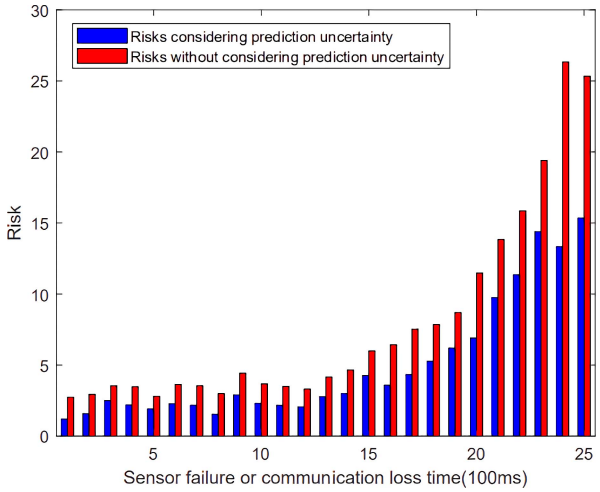

Fig. 13. Risk analysis of lane changing scenario when sensor failure or communication loss.

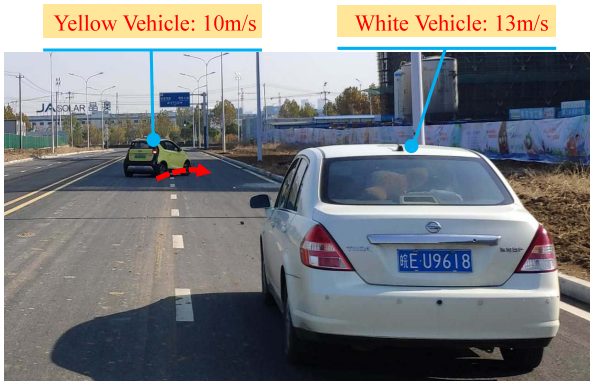

Fig. 14. Imperfect sensing with different accuracies scenario.

failure, a risk assessment considering the risk of uncertainty predicted should be taken into account to ensure higher safety.

3) Situational Assessments Regarding Imperfect Sensing With Different Accuracies: In lane change scenarios, SA in the case of incomplete sensing with different accuracy is investigated. In this case, dynamic Bayesian networks are applied to identify the lane change of yellow vehicle in adjacent lanes [45]. Because the covariance of Gaussian distribution has the ability to represent imperfect perception, Gaussian distribution can be used to represent the perceptual information. For example, as shown in Fig. 14, the yellow vehicle is an intelligent vehicle, and the risk of the white vehicle located in the adjacent lane must be known. First, the yellow vehicle can get relevant information about the white vehicle through on-board sensors. Second, the white vehicle can use communication technology to send relevant information with higher accuracy. Obviously, different sensing accuracy may cause different risks to traffic scenes for yellow vehicle. Therefore, according to different sensing accuracy, this study can obtain uncertainty awareness risks.

The risk analysis of different detection accuracy under lane change is shown in Fig. 15. There are two cases: one is the risks of high detection uncertainty, and the other is the low detection uncertainty of different sensors. As shown in Fig. 15,

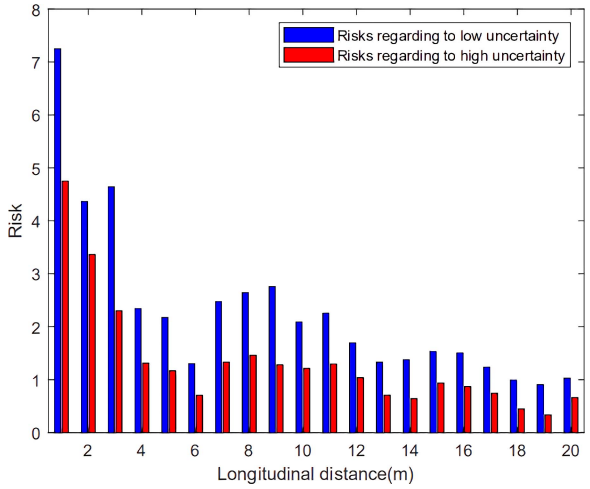

Fig. 15. Risk analysis regarding different detecting accuracies.

the compared results demonstrate that scenario risks might be caused by different sensing uncertainties. The same relative longitudinal distance between a red vehicle and a white vehicle might be a high risk, which could be caused by the high sensing uncertainty. That is, SA is sensitive to the risk of sensing uncertainty. Above results also mean that sensor configurations of IAVs are able to determine the decisionmaking policies, because different sensing capabilities lead to uncertainty risks.

VI. Conclusion

Considering the uncertainty of real-time traffic environment prediction and perception prediction, the SA scheme based on uncertainty risk awareness in real-time traffic environment is proposed. In our study, the risks are evaluated within and outside the prediction range. In the prediction range, the collision risk is assessed via the trajectory prediction under the uncertainty containing the detection uncertainty. The internal energy depends on the weight of the colliding object and the relative speed. Moreover, the final forecast and planning parameters under uncertainty are used to evaluate risks beyond the forecast range. Finally, the SA scheme via uncertainty risk awareness is demonstrated in three scenarios, that is, scenarios with accidental obstacles, sensor failure or communication loss, and incomplete perception with different accuracy.

References

[1] Z. Li, J. Deng, R. Lu, Y. Xu, J. Bai, and C. Su, "Trajectory-tracking control of mobile robot systems incorporating neural-dynamic optimized model predictive approach," *IEEE Trans. Syst. Man Cybern. Syst.*, vol. 46, no. 6, pp. 740–749, Jun. 2016.

[2] Y. Song, X. Wang, G. Wright, D. Thatcher, P. Wu, and P. Felix, "Traffic volume prediction with segment-based regression kriging and its implementation in assessing the impact of heavy vehicles," *IEEE Trans. Intell. Transp. Syst.*, vol. 20, no. 1, pp. 232–243, Jan. 2019.

[3] Z. Li, R. A. Hassan, M. Shahidehpour, S. Bahramirad, and A. Khodaei, "A hierarchical framework for intelligent traffic management in smart cities," *IEEE Trans. Smart Grid*, vol. 10, no. 1, pp. 691–701, Jan. 2019.

[4] J. Scholliers *et al.*, "Development and application of an integrated evaluation framework for preventive safety applications," *IEEE Trans. Intell. Transp. Syst.*, vol. 12, no. 1, pp. 211–220, Mar. 2011.

[5] Q. Wang, P. Fan, and K. B. Letaief, "On the joint V2I and V2V scheduling for cooperative VANETs with network coding," *IEEE Trans. Veh. Technol.*, vol. 61, no. 1, pp. 62–73, Jan. 2012.

[6] P. Dai *et al.*, "Temporal information services in large-scale vehicular networks through evolutionary multi-objective optimization," *IEEE Trans. Intell. Transp. Syst.*, vol. 20, no. 1, pp. 218–231, Jan. 2018.

[7] C. Barrios, Y. Motai, and D. Huston, "Trajectory estimations using smartphones," *IEEE Trans. Ind. Electron.*, vol. 62, no. 12, pp. 7901–7910, Dec. 2015.

[8] J. Zhou, D. Tian, Y. Wang, Z. Sheng, X. Duan, and V. C. M. Leung, "Reliability-optimal cooperative communication and computing in connected vehicle systems," *IEEE. Trans. Mobile Comput.*, vol. 19, no. 5, pp. 1216–1232, May 2020.

[9] C. L. P. Chen, J. Zhou, and W. Zhao, "A real-time vehicle navigation algorithm in sensor network environments," *IEEE Trans. Intell. Transp. Syst.*, vol. 62, no. 12, pp. 1657–1666, Dec. 2012.

[10] Q. Hu, S. Paisitkriangkrai, C. Shen, A. van den Hengel, and F. Porikli, "Fast detection of multiple objects in traffic scenes with a common detection framework," *IEEE Trans. Intell. Transp. Syst.*, vol. 17, no. 4, pp. 1002–1014, Apr. 2016.

[11] X. Li *et al.*, "A unified framework for concurrent pedestrian and cyclist detection," *IEEE Trans. Intell. Transp. Syst.*, vol. 18, no. 2, pp. 269–281, Feb. 2017.

[12] X. Xiong, L. Chen, and J. Liang, "A new framework of vehicle collision prediction by combining SVM and HMM," *IEEE Trans. Intell. Transp. Syst.*, vol. 19, no. 3, pp. 699–710, Mar. 2018.

[13] T. Zhang, X. Wang, X. Xu, and C. L. P. Chen, "GCB-Net: Graph convolutional broad network and its application in emotion recognition," *IEEE Trans. Affect. Comput.*, early access, Aug. 27, 2019, doi: 10.1109/TAFFC.2019.2937768.

[14] D. Tran, W. Sheng, L. Liu, and M. Liu, "A hidden Markov model based driver intention prediction system," in *Proc. IEEE Int. Conf. Cyber Technol. Autom. Control Intell. Syst.*, Shenyang, China, 2015, pp. 115–120.

[15] Z. Duan, Y. Yang, K. Zhang, Y. Ni, and S. Bajgain, "Improved deep hybrid networks for urban traffic flow prediction using trajectory data," *IEEE Access*, vol. 6, pp. 31820–31827, 2018.

[16] L. Wang, L. Zhang, and Z. Yi, "Trajectory predictor by using recurrent neural networks in visual tracking," *IEEE Trans. Cybern.*, vol. 47, no. 10, pp. 3172–3183, Oct. 2017.

[17] D. S. Gonzalez, J. S. Dibangoye, and G. Laugier, "High-speed highway scene prediction based on driver models learned from demonstrations," in *Proc. IEEE 19th Int. Conf. Intell. Transp. Syst.*, Rio de Janeiro, Brazil, 2016, pp. 149–155.

[18] C. Laugier *et al.*, "Probabilistic analysis of dynamic scenes and collision risks assessment to improve driving safety," *IEEE Intell. Transp. Syst. Mag.*, vol. 3, no. 4, pp. 4–19, Oct. 2011.

[19] J. Hillenbrand, A. M. Spieker, and K. Kroschel, "A multilevel collision mitigation approach—Its situation assessment, decision making, and performance tradeoffs," *IEEE Trans. Intell. Transp. Syst.*, vol. 7, no. 4, pp. 528–540, Dec. 2006.

[20] M. Makarov, A. Caldas, M. Grossard, P. Rodríguez-Ayerb, and D. Dumur, "Adaptive filtering for robust proprioceptive robot impact detection under model uncertainties," *IEEE/ASME Trans. Mechatronics*, vol. 19, no. 6, pp. 1917–1928, Dec. 2014.

[21] T. Zhang, G. Su, C. Qing, X. Xu, B. Cai, and X. Xing, "Hierarchical lifelong learning by sharing representations and integrating hypothesis," *IEEE Trans. Syst., Man, Cybern., Syst.*, early access, Feb. 27, 2019, doi: 10.1109/TSMC.2018.2884996.

[22] Y. Zhang, Q. Lin, J. Wang, S. Verwer, and J. M. Dolan, "Lane-change intention estimation for car-following control in autonomous driving," *IEEE Trans. Intell. Veh.*, vol. 3, no. 3, pp. 276–286, Sep. 2018.

[23] J. Suh, H. Chae, and K. Yi, "Stochastic model-predictive control for lane change decision of automated driving vehicles," *IEEE Trans. Veh. Technol.*, vol. 67, no. 6, pp. 4771–4782, Jun. 2018.

[24] A. Goswami, "Trajectory generation for lane-change maneuver of autonomous vehicles," Ph.D. dissertation, Dept. Elect. Comput. Eng., Purdue Univ., West Lafayette, IN, USA, 2015.

[25] M. Li, H. Cao, X. Song, Y. Huang, J. Wang, and Z. Huang, "Shared control driver assistance system based on driving intention and situation assessment," *IEEE Trans. Ind. Informat.*, vol. 14, no. 11, pp. 4982–4994, Nov. 2018.

[26] T. Sato and M. Akamatsu, "Influence of traffic conditions on driver behavior before making a right turn at an intersection: Analysis of driver behavior based on measured data on an actual road," *Transp. Res. F, Traffic Psychol. Behav.*, vol. 10, no. 5, pp. 397–413, Sep. 2007.

[27] J. Lee, B. B. Park, K. Malakorn, and J. So, "Sustainability assessments of cooperative vehicle intersection control at an urban corridor," *Transp. Res. C, Emerg. Technol.*, vol. 32, pp. 193–206, Jul. 2013.

[28] M. Lee, M. Sunwoo, and K. Jo, "Collision risk assessment of occluded vehicle based on the motion predictions using the precise road map," *Robot. Auton. Syst.*, vol. 106, pp. 179–191, Aug. 2018.
[29] M. Tanelli, R. Toledo-Moreo, and L. M. Stanley, "Guest Editorial: Multifaceted driver–vehicle systems: Toward more effective driving simulations, reliable driver modeling, and increased trust and safety," *IEEE Trans. Human-Mach. Syst.*, vol. 48, no. 1, pp. 1–5, Feb. 2018.
[30] J. Wang, J. Wu, and Y. Li, "The driving safety field based on driver–vehicle–road interactions," *IEEE Trans. Intell. Transp. Syst.*, vol. 16, no. 4, pp. 2203–2214, Aug. 2015.
[31] W. Wang, J. Xi, and D. Zhao, "Learning and inferring a driver's braking action in car-following scenarios," *IEEE Trans. Veh. Technol.*, vol. 67, no. 5, pp. 3887–3899, May 2018.
[32] D. Yi, J. Su, C. Liu, and W.-E. Chen, "Trajectory clustering aided personalized driver intention prediction for intelligent vehicles," *IEEE Trans. Ind. Informat.*, vol. 15, no. 6, pp. 3693–3702, Jun. 2019.
[33] K. Kim, K. Lee, B. Ko, B. Kim, and K. Yi, "Design of integrated risk management-based dynamic driving control of automated vehicles," *IEEE Intell. Transp. Syst. Mag.*, vol. 9, no. 1, pp. 57–73, Jan. 2017.
[34] J. R. Ward, G. Agamennoni, S. Worrall, A. Bender, and E. Nebot, "Extending time to collision for probabilistic reasoning in general traffic scenarios," *Transp. Res. C, Emerg. Technol.*, vol. 51, pp. 66–82, Feb. 2015.
[35] B. Kim, K. Park, and K. Yi, "Probabilistic threat assessment with environment description and rule-based multi-traffic prediction for integrated risk management system," *IEEE Intell. Transp. Syst. Mag.*, vol. 9, no. 3, pp. 8–22, Jul. 2017.
[36] J. Jansson and F. Gustafsson, "A framework and automotive application of collision avoidance decision making," *Automatica*, vol. 44, no. 9, pp. 2347–2351, Sep. 2008.
[37] M. Schreier, V. Willert, and J. Adamy, "An integrated approach to maneuver-based trajectory prediction and criticality assessment in arbitrary road environments," *IEEE Trans. Intell. Transp. Syst.*, vol. 17, no. 10, pp. 2751–2766, Oct. 2016.
[38] E.-Y. Lee, H.-J. Cho, and K.-Y. Ryu, "A probabilistic approach for collision avoidance of uncertain moving objects within black zones," *Ad Hoc Netw.*, vol. 52, pp. 50–62, Dec. 2016.
[39] A. Houénou, P. Bonnifait, and V. Cherfaoui, "Risk assessment for collision avoidance systems," in *Proc. IEEE 17th Int. Conf. Intell. Transp. Syst.*, Qingdao, China, 2014, pp. 386–391.
[40] D. I. Katzourakis, J. C. F. de Winter, M. Alirezaei, M. Corno, and R. Happee, "Road-departure prevention in an emergency obstacle avoidance situation," *IEEE Trans. Syst., Man, Cybern., Syst.*, vol. 44, no. 5, pp. 621–629, May 2014.
[41] C. Barrios, Y. Motai, and D. Huston, "Intelligent forecasting using dead reckoning with dynamic errors," *IEEE Trans. Ind. Informat.*, vol. 12, no. 6, pp. 2217–2227, Dec. 2016.
[42] H. B. Gao, T. L. Zhang, Y. C. Liu, and D. Y. Li, "Research of intelligent vehicle variable granularity evaluation based on cloud mode," *Acta Electronica Sinica*, vol. 44, no. 2, pp. 365–374, 2016.
[43] D. Y. Li and H. B. Gao, "A hardware platform framework for an intelligent vehicle based on a driving brain," *Engineering*, vol. 4, no. 4, pp. 464–470, 2018.
[44] D. Althoff, J. J. Kuffner, D. Wollherr, and M. Buss, "Safety assessment of robot trajectories for navigation in uncertain and dynamic environments," *Auton. Robot.*, vol. 32, no. 3, pp. 285–302, Apr. 2012.
[45] G. T. Xie, H. B. Gao, B. Huang, L. Qian, and J. Wang, "A driving behavior awareness model based on a dynamic Bayesian network and distributed genetic algorithm," *Int. J. Comput. Intell. Syst.*, vol. 11, no. 1, pp. 469–482, 2018.

Hongbo Gao received the Ph.D. degree in computer science and technology from Beihang University, Beijing, China, in 2016.

He is currently an Associate Professor with the Department of Automation, School of Information Science and Technology, University of Science and Technology of China, Hefei, China. He has authored or coauthored over 30 journal papers, and he is the co-holder of 6 patent applications. His current research interests include unmanned system platform and robotics, machine learning, decision support system, and intelligent driving.

Juping Zhu received the B.S. degree in mathematics from Anhui University, Hefei, China, in 2020. She is currently pursuing the M.S. degree in control engineering with the University of Science and Technology of China, Hefei.

Her current research interests include intelligent driving and risk situation assessment.

Tong Zhang (Member, IEEE) received the B.S. degree in software engineering from Sun Yat-sen University, Guangzhou, China, in 2009, and the M.S. degree in applied mathematics from University of Macau, Macau, China, in 2011, and the Ph.D. degree in software engineering from the University of Macau, Macau, in 2016.

He currently is an Associate Professor with the School of Computer Science and Engineering, South China University of Technology, Guangzhou, China, and the Pazhou Lab, Guangzhou. His research interests include affective computing, evolutionary computation, neural network, and other machine learning techniques and their applications. He has been working in publication matters for many IEEE conferences.

Guotao Xie received the bachelor's and doctor's degrees in automotive engineering from the Hefei University of Technology, Hefei, China, in 2013 and 2018, respectively.

He was also a joint student of the State Key Laboratory of Automotive Safety and Energy, Tsinghua University, Beijing, China, from 2013 to 2018. From 2016 to 2017, he was a visiting student with the Department of Electrical and Computer Engineering, Ohio State University, Columbus, OH, USA. He is currently an Associate Research Fellow with Hunan University, Changsha, China. His current research interests include connected and automated vehicles, environment perception, situational awareness, and environment prediction.

Zhen Kan (Member, IEEE) received the Ph.D. degree in mechanical and aerospace engineering from the Department of Mechanical and Aerospace Engineering, University of Florida, Gainesville, FL, USA, in 2011.

He is a Professor with the Department of Automation, University of Science and Technology of China, Hefei, China. He was a Postdoctoral Research Fellow with the Air Force Research Laboratory, Eglin AFB and University of Florida REEF, Shalimar, FL, USA, from 2012 to 2016, and was an Assistant Professor with the Department of Mechanical Engineering, University of Iowa, Iowa City, IA, USA. His current research interests include networked robotic systems, Lyapunov-based nonlinear control, graph theory, complex networks, and human-assisted estimation, planning, and decision making.

Prof. Kan currently serves as an Associate Editor on Conference Editorial Board in the IEEE Control Systems Society and technical committee for several internationally recognized scientific and engineering conferences.

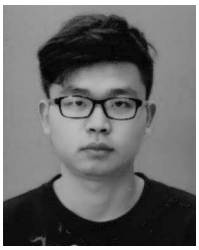

Zhengyuan Hao received the B.S. degree in automation from Shandong University, Jinan, China, in 2019. He is currently pursuing the M.S. degree in control engineering with the University of Science and Technology of China, Hefei, China.

His current research interest includes autonomous driving.

Kang Liu received the B.S. degree in automation engineering from the Department of Automation, Donghua University, Shanghai, China, in 2017. He is currently pursuing the Ph.D. degree with the Department of Automation, University of Science and Technology of China, Hefei, China.

His current research interests include intelligent driving, artificial intelligence, and adaptive control.